

POWER MODULATION MODELING OF ALUMINUM REDUCTION CELLS FOR RENEWABLE ENERGY INTEGRATION

Gustavo Ospina-Aldana¹, Mohamed I. Hassan Ali², Sgouris Sgouridis¹, Ali Bouabid¹

¹ Khalifa University of Science and Technology

² Khalifa University of Science and Technology (Corresponding Author)

ABSTRACT

This paper presents the development of a thermodynamic model to determine the extended operating window of an aluminum cell to enable power modulation. The integration of renewable energy to aluminum production needs to overcome the challenge of narrow operating windows of aluminum cells. The proposed model takes an industrial aluminum cell as a case study to demonstrate how to build the operating window, constrained by the cell design technical limitations. The extended operating window can also be used to estimate the heat exchanger heat rate requirements to enable an aluminum cell to operate under a wide power modulation.

Keywords: Aluminum production, energy transition, power modulation, renewable energy.

NOMENCLATURE

Abbreviations	
ACD	Anode-to-cathode distance
CD	Current density
CE	Current efficiency
SEC	Specific energy consumption
UAE	United Arab Emirates

1. INTRODUCTION

Aluminum is an important metal for the energy transition. It's the most abundant metal on the earth's crust and its lightweight, corrosion resistance, and high thermal and electrical conductivity makes aluminum range of application very wide. Aluminum is widely used in construction, aerospace, marine, rail and primarily the automotive industry. Aluminum use will likely increase, as tighter emissions regulations push its wider adoption into lighter vehicles. However, the production of aluminum is highly energy intensive.

The total primary aluminum energy consumption in 2017 was 863.3 TWh, 3.38% of global electricity demand [1]. The aluminum energy intensity production varies by the state of technology used and can be a significant component of the country's demand. In the UAE, the aluminum industry requires 20% of the total installed electricity generation capacity of the country.

Aluminum cells are operated within a narrow power input operating window to achieve a target bath operating temperature between 955 °C and 970 °C, this temperature range provides the best operating conditions for an aluminum cell [2]. To keep aluminum cells within this narrow operating range, operations prefer constant power.

Selection and peer-review under responsibility of the scientific committee of the 11th Int. Conf. on Applied Energy (ICAE2019).

One of the first technologies to enable aluminum cell power modulation is Enpot [3]. Using a shell heat exchanger, an aluminum cell can reject a larger excess heat staying within the target bath temperature, allowing higher energy inputs. On the other hand, if a lower power input is to be given to the cell, the shell wall heat exchanger provides an additional insulation enabling the use of lower power inputs while staying above the minimum target cell temperature.

The first component that is needed on a power modulation study is a model of the aluminum cell to simulate the performance of the cell under several power modulation schemes. Such a model can be used to optimize the power modulation curves constrained by technical parameters of the cell in addition to costs constraints. The model also needs to provide the input data to size a heat exchanger for the aluminum cell. This paper develops an aluminum cell model that is able to investigate its thermal properties and transient heat behavior during modulation. Specifically the cell model provides at steady state and for a given power input: aluminum production, SEC, and total heat loss at steady state. These allow to estimate:

1. Minimum and maximum power input for an aluminum cell corresponding to the minimum and maximum target bath temperatures without any modification to an existing design (basic case).
2. Heat extraction rate required to increase the aluminum cell power input by a prescribed amount beyond the basic case maintaining the temperature at the maximum target.
3. Additional insulation required to reduce the power by a prescribed amount maintaining the temperature at the minimum target.
4. Suitable ACD variations through the power modulation cycle to reduce the heat exchanger load.

2. MATERIALS AND METHODS

2.1 Case study

Emirates Global Aluminum (EGA) is the world's largest 'premium aluminum' producer and the 5th largest aluminum producer in the world by total aluminum

production with a production of 2.6 million tonnes of aluminum in 2017. EGA's energy supply is provided by its own gas power plants with a total installed capacity of 5.45 GW which is approximately 20% of the total installed capacity of the UAE. Currently, EGA produces aluminum using constant power input.

The latest aluminum reduction cell technology implemented by EGA is called DX+ Ultra. This cell was used as the case study to illustrate the development of a thermodynamic model to determine the power modulation boundaries for an aluminum cell.

The following are the main operating parameters of the EGA DX+ Ultra cell. The full set of input parameters was collected from [4]. Each reduction cell requires a nominal power of 1855.58 kW. There are currently 444 cells with this technology at EGA's plants, which consume a total combined power of 823.9 MW.

Table 1 EGA DX+ Ultra main operating parameters [4].

Parameter	Value
Current [kA]	454.8
Voltage [V]	4.08
Current efficiency [%]	95.0
SEC [kWh/kg Al]	12.8
Aluminum production [kg/cell-day]	3479

2.2 Thermodynamic model

A thermodynamic energy balance is required to determine the heat loss from the cell. The voltage component on the energy balance is decomposed in voltage drops across the cell: from entry to anode, from the electrolyte and the cathode to exit voltage drop. These voltage drops occur in solid materials, which are the structural materials of the cell conducting electricity and the anode and cathode. Voltage drops are also calculated on liquid and gas substances. Gas bubbles are formed under the anode introducing an additional electric resistance. Depending on the chemical composition of the electrolyte molten bath, the resistivity of the bath varies. All the necessary equations to calculate the different voltage drops across the cell were collected from literature, and the full set of

equations was coded in Matlab. The model used EGA's DX+ Ultra aluminum cell [4] as a case study.

The basic input data for the thermodynamic model is the current, anode-to-cathode distance (ACD), current efficiency number of anodes and anode geometry, bath temperature and chemical composition, entry to anode components electric resistance (i.e. riser, flexibles, clamp, anode rod, anode block), and cathode to exit components electric resistance (i.e. cathode block, flexibles, busbar, riser) and anode gas bubble fraction. The model key outputs are the cell voltage, aluminum production, specific energy consumption and total heat loss. The main result expected from the model is the aluminum cell extended power modulation window.

The power modulation operating window will be defined by the following parameter values:

- Minimum and maximum target ACD

The model estimates the ACD that generates the voltage drop reported at the nominal operating point. The minimum ACD is a hard constraint that represents the minimum possible distance that can be achieved in the current cell design. The maximum target ACD is chosen from the electrolyte bath height and anode height to ensure there is sufficient anode immersion depth.

- Minimum and maximum heat loss

The maximum and minimum heat loss beyond the nominal heat loss were defined reviewing the performance of an industrial tested shell heat exchanger (SHE) for an aluminum cell that can remove excess heat and provide additional insulation. The performance limits of the SHE allow an operation with a heat loss $\pm 12\%$ from the nominal point [2].

- Minimum cathode current density

In aluminum cells, there is a sharp drop in current efficiency at low current densities. The curve of current efficiency loss as function of cathode current density (CD) is cell design specific and determined experimentally. However for this study, the onset value

for current efficiency loss (0.7 A/cm^2) was estimated with data from [5].

2.3 Thermal energy storage calculation

Following the approach and assumptions presented by [2], calculating the energy stored in the aluminum cell at the two limit target temperatures, $955 \text{ }^\circ\text{C}$ and $970 \text{ }^\circ\text{C}$, gives an estimate of the power input limits on an aluminum cell without heat exchangers. This requires the temperature distribution in the cell at the two states, the mass of all materials in the cell and their corresponding temperature dependent heat capacities must be known, to calculate the thermal energy stored in the cell applying equation 1, with the ambient temperature 25°C used as reference for the temperature change:

$$Q = \sum mc_p \Delta T \quad (1)$$

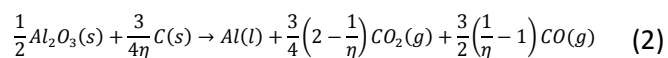
The temperature distribution on the aluminum cell was calculated using a validated steady state heat transfer FEM model presented by [6].

The temperature dependent heat capacities of all the materials in the aluminum cell were calculated using the corresponding Shomate equations and the schematic cell cross section and its constitutive materials [6]. The coefficients of the Shomate equation for all the aluminum cell materials can be found in [7-9]. Industrial testing has been conducted by previous authors to validate this approach, modulating the power by 30% of the calculated energy difference with overall good cell performance [10].

3. THEORY

3.1 Thermodynamic model equations

The thermodynamic model uses the following aluminum production reaction, which considers a loss in current efficiency due to back reaction, or reoxidation of a fraction $(1 - \eta)$ of the produced aluminum. For modern cells, the fractional current efficiency $\eta = 0.95$:



The first law analysis of an aluminum cell yields:

$$\dot{W}_{el} + \Sigma \dot{n}_{Al} \bar{h}_r = \dot{Q} + \Sigma \dot{n}_{Al} \bar{h}_p \quad (3)$$

Where \dot{W}_{el} is the electric power input ($I \cdot V_{cell}$), \dot{n}_{Al} is the molar rate of aluminum, \bar{h}_r and \bar{h}_p are the specific enthalpy per mole of reactants and products respectively, from the aluminum production reaction (equation 2) and \dot{Q} is the heat loss. For the enthalpy calculation, it was considered that the reactants are first heated to the bath temperature from ambient temperature. The bath temperature in aluminum electrolysis is typically between 955 °C and 970 °C.

The first law energy balance can be rearranged to obtain the SEC term in kWh/kg Al which is commonly used in the aluminum industry:

$$\frac{\dot{W}_{el}}{\dot{m}_{Al}} - \frac{10}{36M_{Al}} (\Sigma \bar{h}_p - \Sigma \bar{h}_r) = \frac{\dot{Q}}{\dot{m}_{Al}} \quad (4)$$

Where M_{Al} is the aluminum molar mass in (kg/kmol), \bar{h}_r and \bar{h}_p are specific enthalpies for reactants and products respectively in kJ/mol and $\frac{\dot{W}_{el}}{\dot{m}_{Al}}$ and $\frac{\dot{Q}}{\dot{m}_{Al}}$ are the specific energy consumption and specific heat loss respectively, in kWh/kg Al.

3.2 Aluminum cell voltage drop equations

To calculate the voltage drop between the entry and the anode $V_{entry-anode}$ on equation 5, the electric resistance of each component of the anode assembly was estimated from corresponding published voltage drop at a known operating current [11].

$$V_{cell} = V_{entry-anode} + V_{cath-exit} + V_{bath} \quad (5)$$

Similarly to the entry to anode voltage drops, the electric resistance of the components was estimated from literature data of voltage drops and operating current. The cathode to exit components considered for resistance calculation were the cathode block, flexibles, busbar and riser with data from [12].

The bath voltage V_{bath} is composed of the voltage drops across the anode to cathode distance shown in equation 6.

$$V_{bath} = V_{bub} + V_{ACD} + E_e + V_{ra} + V_{sa} + V_{cc} \quad (6)$$

The bubbles voltage drop V_{bub} occurs due to the configuration of the aluminum cell, where the anode is placed horizontally with its biggest surface facing down, causes the carbon oxide gases produced during the electrolysis to accumulate on the anode surface creating a bubbles layer. The bubbles layer acts as an insulator for the electric current flowing through the anode to the bath producing the bubbles voltage drop. To calculate the bubble voltage drop, the necessary inputs are the bubbles layer thickness, bubble fraction coverage and the anode side current fraction, to get the actual current flowing vertically.

As a reference, the steady state gas layer thickness of a 300 kA cell with slotted anodes described on [13] is approximately 16 mm. The bubble fraction of the EGA DX+ Ultra cell is reportedly 0.5, from industrial experience [14]. The equations to obtain the anode side current fraction and the total bubbles voltage drop V_{bub} can be found in [15].

The electrolyte voltage drop V_{ACD} is caused by the current flow between anode and cathode against the electric resistance of the bath electrolyte. The electric resistance of the bath electrolyte is a function of the cell temperature and the chemical composition. To calculate the bath electric resistance, the equation in [16] was used. The necessary bath composition inputs were collected from [4].

$$E_e = E^o + \frac{RT}{12F} \ln \frac{a_{Al}^4 a_{CO_2}^3}{a_{Al_2O_3}^4 a_C^3} \quad (7)$$

Equation 7 represents the equilibrium potential, E_e , at cell operating temperature and species concentrations, a_{Al} , a_{CO_2} , $a_{Al_2O_3}$ and a_C . E^o is the standard potential at 25 °C and 1M. Previous authors have noted that the activities of Al, CO₂ and C in aluminum cells are close enough to their standard states that they can be assumed to be unit value. However the same assumption cannot be made for alumina. This value must be measured. A fitting equation can be found in literature to calculate the alumina activity [17].

The reversible decomposition voltage or standard potential equivalent to E^o is the minimum voltage that

needs to be provided to an ideal electrolysis cell, according to the ideal aluminum electrolysis reaction (Eq. 2) with ($\eta = 1$). Using the Gibbs Free energy change of the ideal electrolysis reaction (Eq. 2), and combining the Faraday's Law, the standard potential can be calculated with the following equation:

$$E^{\circ} = \frac{\Delta G}{nF} \quad (8)$$

Where F is the Faraday's constant, n is the number of free electrons and ΔG is the Gibbs free energy change of Eq. 2 reaction with $\eta=1$.

In order for the electrolysis reaction to occur at an appropriate speed, an additional voltage must be supplied. The anodic reaction overvoltage (V_{ra}), anodic concentration overvoltage (V_{sa}) and cathodic concentration overvoltage (V_{cc}) equations can be found in [18].

3.2.1 Aluminum production and SEC

The equation to calculate aluminum production by electrolysis is derived from the Al^{3+} to Al (s) half-reaction. The Faraday's constant ($F=96485.33$ s A/mol) allows to calculate the number of moles of electrons that will pass through the cell for a given charge. The electric charge is simply the product of current and time ($1\text{ C}=1\text{ A}\cdot\text{s}$). Using the aluminum molar weight, the specific aluminum production per day \dot{m}_{Al} can be obtained. The fractional current efficiency term η is introduced to account for the aluminum back-reaction.

$$\dot{m}_{Al} = 8.0537 \cdot I \cdot \eta \text{ kg/kA-day} \quad (9)$$

The aluminum specific energy consumption (SEC) is calculated as the ratio of the energy input ($I \cdot V_{cell}$) over the specific aluminum production rate \dot{m}_{Al} .

4. RESULTS

4.1 Thermal energy storage calculation

The thermal energy storage calculation sheet was validated using the data presented in [10]. The error was less than 1%. Analyzing the EGA DX+ Ultra cell, which operates at a nominal point of 454.8 kA and 4.08 V, it was found that the energy stored at 955 °C is approximately

49.89 MWh while the energy stored in the cell at 970 °C is approximately 54.18 MWh.

There is an energy difference of 4.29 MWh between the target temperatures. This value is needed to estimate the maximum duration of a given power input modulation cycle without adding heat exchangers. Using a conservative approach from previous industrial tests presented in [10], only 30% of the calculated energy difference will be considered

Using the thermal energy storage calculation, it was estimated that the power input to the cell can be increased by 8% from the nominal value (up to 477.2 kA, 4.2 V, at ACD 3.4cm) for approximately 8.5 hours, followed by a 8% power reduction (down to 432.1 kA, 3.9 V, at ACD 3.4cm) for approximately 4.3 hours.

4.2 Thermodynamic model

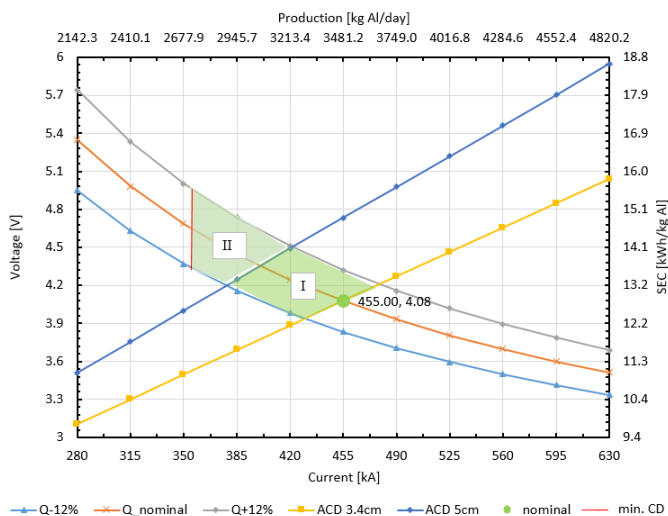
The specific energy consumption and aluminum production of the cell at the rated point of 454.8 kA and 4.08 V[4] were calculated with the model within 2% error from the published industrial data. The thermodynamic model was used to build the steady state power modulation window of EGA's aluminum cell. The usage of a shell heat exchanger can allow the aluminum production to be modulated between -16.9% and +5.2% from the nominal production rate (3481 kg Al/day). This production range can be achieved with a power modulation between -14.5% and +8.6% from the nominal power (1855.2 kW).

This modulation scheme can be performed at a nearly constant SEC of 13.2 kWh/kg Al, within region I, bounded by an ACD between 3.4 cm and 5 cm (Figure 1). A further production modulation can be achieved getting into region II reaching the lower limit of current density, however, reducing the current below this limit will start to reduce the current efficiency of the process.

5. CONCLUSION

The power and production of an aluminum cell can be controlled over a wide range by controlling the heat losses from the side walls. Controlling the heat losses of an aluminum cell enables the adaptation of aluminum

production to fluctuations in energy supply and also it can give aluminum smelters the capacity to adjust production. The definition of the power modulation boundaries was illustrated considering the latest aluminum cell design in the UAE.



ACKNOWLEDGEMENT

This publication is based upon work supported by the Khalifa University of Science and Technology under Award No. CIRA-2018-97.

REFERENCES

[1] Dudley, B., 2018, "BP statistical review of world energy 2018," British Petroleum BP, London, UK.

[2] Carsten Reek, T., 2015, "Power Modulation of Aluminium Reduction Cells – Operational Constraints and Process Limits," University of New South Wales, Sydney, Australia.

[3] Depree, N., Düssel, R., Patel, P., and Reek, T., 2016, "The 'Virtual Battery' – Operating an Aluminium Smelter with Flexible Energy Input," Light Metals 2016, E. Williams, ed., Springer International Publishing, Cham, pp. 571-576.

[4] Alzarouni, A., Alzarooni, A., Ahli, N., Akhmetov, S., and Arkhipov, A., "DX+ Ultra—EGA High Productivity, Low Energy Cell Technology," Springer International Publishing, pp. 769-774.

[5] Solli, P. A., Eggen, T., Skybakmoen, E., and Sterten, Å., 1997, "Current efficiency in the Hall–Héroult process for aluminium electrolysis: experimental and modelling studies," Journal of Applied Electrochemistry, 27(8), pp. 939-946.

[6] Brimmo, A. T., Hassan, M. I., and Shatilla, Y., 2014, "Transient heat transfer computational model for the stopped aluminium reduction pot – Cooling techniques

evaluation," Applied Thermal Engineering, 73(1), pp. 116-127.

[7] Chase Jr, M., 1998, "NIST-JANAF thermochemical tables fourth edition," J. Phys. Chem. Ref. Data, Monograph, 9.

[8] Anovitz, L. M., Hemingway, B. S., Westrum Jr, E. F., Metz, G. W., and Essene, E. J., 1987, "Heat capacity measurements for cryolite (Na₃AlF₆) and reactions in the system Na-Fe-Al-Si-O-F," Geochimica et Cosmochimica Acta, 51(12), pp. 3087-3103.

[9] Don, W. G., and Robert, H. P., 2008, "Specific heats of pure compounds," Perry's Chemical Engineers' Handbook, Eighth Edition, McGraw Hill Professional, Access Engineering.

[10] Reek, T., 2016, "New approaches to power modulation at TRIMET Hamburg," Light Metals 2011, S. J. Lindsay, ed., Springer International Publishing, Cham, pp. 375-379.

[11] Arkhipov, A., "Review of Thermal and Electrical Modelling and Validation Approaches for Anode Design in Aluminium Reduction Cells," Proc. Proceedings of 36th International ICSOBA Conference, Travaux No. 47, Belem, Brazil.

[12] Mishra, L. K., Anwar, M., Arkhipov, A., Aljasmii, A., Ahli, N., Alzarooni, A., and Al Jaziri, A., "New connections for cathode flexibles in aluminium electrolysis cells," Proc. Proceedings of 35th International ICSOBA Conference, Travaux No.

[13] Sun, M., Li, B., Li, L., Wang, Q., Peng, J., Wang, Y., and Cheung, S. C. P., 2017, "Effect of Slotted Anode on Gas Bubble Behaviors in Aluminum Reduction Cell," Metallurgical and Materials Transactions B, 48(6), p. 3161.

[14] Peng, C.-Y., Lan, C.-H., Lin, P.-C., and Kuo, Y.-C., 2017, "Effects of cooking method, cooking oil, and food type on aldehyde emissions in cooking oil fumes," Journal of Hazardous Materials, 324, Part B, pp. 160-167.

[15] Zoric, J., Roušar, I., and Thonstad, J., 1997, "Mathematical modelling of industrial aluminium cells with prebaked anodes: Part I: Current distribution and anode shape," Journal of Applied Electrochemistry, 27(8), p. 916.

[16] Hiveš, J., Thonstad, J., Sterten, Å., and Fellner, P., 1996, "Electrical conductivity of molten cryolite-based mixtures obtained with a tube-type cell made of pyrolytic boron nitride," Metallurgical and Materials Transactions B, 27(2), pp. 255-261.

[17] Skybakmoen, E., Solheim, A., and Sterten, Å., 1997, "Alumina solubility in molten salt systems of interest for aluminum electrolysis and related phase diagram data," Metallurgical and Materials Transactions B, 28(1), p. 81-86.

[18] Haupin, W., 2016, "Interpreting the Components of Cell Voltage," Essential Readings in Light Metals: Volume 2 Aluminum Reduction Technology, G. Bearne, M. Dupuis, and G. Tarcy, eds., Springer International Publishing, Cham, pp. 153-159.